Investigation on the Time-Variant Flow in a Single-Blade Centrifugal Pump

FRIEDRICH-KARL BENRA, HANS JOSEF DOHMEN
Faculty of Engineering Sciences
Department of Mechanical Engineering, Turbomachinery
University of Duisburg-Essen
Lotharstr. 1, 47048 Duisburg, Germany

Abstract: - Effects of the time-variant flow in a single-blade pump are investigated by numerical and experimental methods. For a numerical approach the three-dimensional, viscous, unsteady flow field in the pump has been achieved by solving the unsteady Navier-Stokes equations (URANS) with a commercial solver. From the obtained periodic flow field the time-variant forces acting at the wetted impeller surface were determined for a complete impeller revolution. To validate the results of the numerical simulations a test stand has been used. The velocity field inside the pump has been measured by using the PIV method. A good comparison to the numerical simulations has been achieved. In a second step the forces acting at the bearings of the pump rotor have been measured. To identify the transient radial forces, the pump has been fitted with special manufactured seats for the roller bearings, which have been equipped with strain gages. The experimental results match the numerical results for the hydrodynamic forces very good. In particular, the good qualitative agreement suggests that predicting the transient flow in (single-blade) centrifugal pumps utilizing a Navier-Stokes solver, is a reliable method to calculate the time-variant hydrodynamic forces.
Key-Words: - Time-variant flow, centrifugal pump, single-blade impeller

1 Introduction

The examination of the flow field in pumps in general can be achieved by analytical, numerical and experimental methods. Because of the complexity of the pump geometry the flow field normally has strong variations of all parameters in all three coordinate directions. Additionally, due to the rotating impeller the flow is strictly transient. The time-variant flow in pumps with a single-blade impeller results in periodic unsteady flow forces which affect the impeller and which produce strong radial deflections of it [1-3]. The known analytical methods are unable to predict such a flow field with the required accuracy. Numerical methods solving the Reynolds Averaged Navier-Stokes equations have been developed to powerful tools in the past decade. Combined with the available computer hardware substantial numerical solutions for complex flow fields can be realized in a time-consuming and cost saving way even for time-variant flows. But the question which has to be placed is: What about the quality of the results and how reliable are the solutions? This question only can be answered when the results of the fluid mechanical problem are known a priori or by using a complete different examination method for validation. This leads to an experimental evaluation method, which in most cases is more costly and time-consuming than a numerical method. But it can show the real behavior because nearly no assumptions and simplifications are accomplished. A disadvantage of the experiments is that for the evaluation of divers flow parameters often completely different tests are necessary.

2 Numerical Investigation

A numerical determination of the flow in a centrifugal pump requires a model, in which beside the outer boundaries of the computing area also the spatial discretization of the flow area is described. On the basis of a volume model of the pump in the parametric CAD system ProEngineer the flow area was discretized by a block-structured computing grid with the grid generator Ansys ICEM CFD. Since neither the impeller nor the casing possessed a plane of symmetry, a complete meshing of the fluid volume for all components was necessary. The grid of the impeller contained 68 blocks with approximately 884000 grid points, while for the casing 27 blocks with approximately 338000 grid points were generated. The grids of both the hub and the shroud side chambers between the impeller discs and the casing walls were created together with the grid of the impeller. In this way the leakage flow from pressure side to suction side has been incorporated in the analysis. The grids of the impeller and the casing were attached to each other by a general interface at a cylindrical surface, which allows the grid of the impeller to rotate in the casing (sliding mesh). The independence of the solutions from the number of grid nodes has been proven by simulating the flow field with different numbers of grid nodes. The non-dimensional distance of the first grid nodes to the wall (y+-values) was below 100 in the complete flow field.
In figure 1 the numerical model of the single-blade pump is depicted. In addition some details of the computational grid at the leading edge and at the trailing edge are

ISSN: 1790-5117

ISBN: 978-960-6766-30-5

given. The restrictions for the numerical simulation were: Second order spatial discretization, second order backward time discretization, turbulence model: k-ω SST model with near wall description.

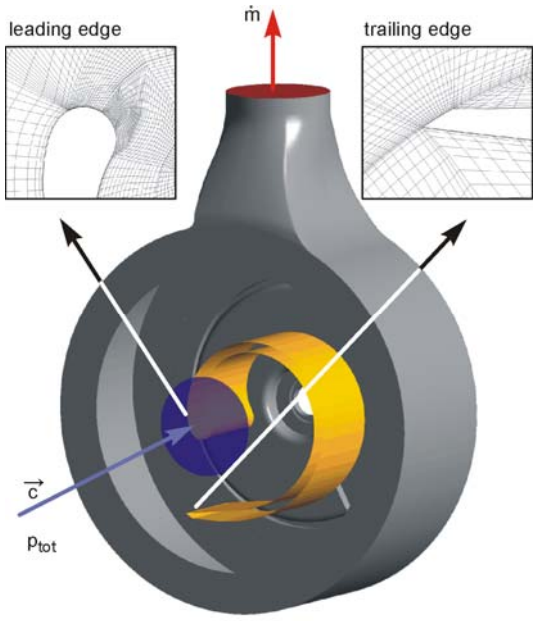

Figure 1: Numerical model of single-blade pump

The time step for the transient simulations has been calculated from equ. (1) using an impeller turning angle of $\Delta\varphi$ = 3 deg. This time step has been proven to be small enough to resolve the periodic flow. Additional information about the numerical simulation procedure can be taken from [4 and 5].

$$\Delta t = \frac{\Delta\varphi \cdot \pi}{180|\omega|} \qquad (1)$$

To answer the question if the behavior of the flow field depends on the boundary conditions, which usually are prescribed as constant values (pressure and mass flow) at the inlet flange and at the outlet flange of the pump, a new simulation model has been developed for this pump. This new model treats the pump as a closed loop. The same spatial discretization has been used for the pump, but to overcome the constant total pressure at the inlet flange and the constant flow rate at the outlet flange of the pump a pipe has been attached at the pressure flange which includes a loss module. Behind the loss module the pipe meets the inlet flange of the pump building a closed loop (see figure 2).

For this closed loop model no boundary conditions must be given. The mass flow and the total pressure of the pump were calculated during the simulation and they varied with the impeller turning angle. The time averaged mass flow has been fitted by varying the loss coefficient of the loss module in several approaches. When the computed time-averaged mass flow met the amount of the flow rate under investigation the loss coefficient has been regarded as well adjusted.

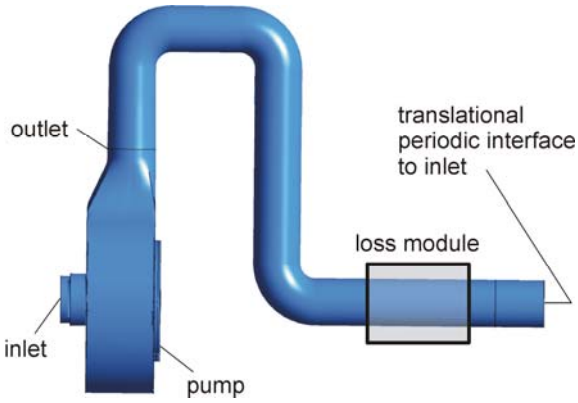

Figure 2: Scheme of the closed loop model

Usually both normal and tangential stresses act on the surface of a body in a flow field. When the flow field affecting the pump impeller is known from the numerical simulation, the pressure forces can be calculated from the normal stresses and the friction forces from the tangential stresses. An integration of the pressure field along the wetted surface of the impeller gives the resulting pressure force vector according to equation (2):

$$\vec{F}_p = -\int p \cdot \vec{e}_n \cdot dA \qquad (2)$$

The friction at the wetted impeller surface leads to a wall stress, which gives an additional force fraction. The resulting friction force vector can be calculated by evaluating equation (3):

$$\vec{F}_f = -\mu \int \frac{d\vec{v}}{dn} \cdot \vec{e}_n \cdot dA \qquad (3)$$

It has been proven that the pressure forces exceed the friction forces by several orders of magnitudes [6]. The integration over the complete impeller surface results in the forces affecting the impeller for each time step. The components of the hydrodynamic forces perpendicular to the shaft axis are crucial for the stimulation of bending vibrations, since they cause a deflection of the shaft in radial direction. So they are called the radial forces. The components in axial direction give the axial thrust of the impeller. The complete hydrodynamic force can be obtained by summarizing both the pressure and the friction part of the forces for each time step:

$$\vec{F}_{rad} = \vec{F}_p + \vec{F}_f \qquad (4)$$

3 Experimental Investigation

To validate the results of the CFD method, measurements have been accomplished at a test stand which originally has been constructed under the guidance of Prof. Siekmann at Technical University of Berlin [7]. In figure 3 a schematic view of the test facility is shown. It contains a vertical arranged submersible single-blade pump which is powered by an electric motor with constant speed of rotation. The motor drives a cardan shaft which is connected to the pump shaft. This pump was particularly designed for that test

ISSN: 1790-5117

ISBN: 978-960-6766-30-5

facility in order to measure the velocity fields in the pump by optical methods. So the single-blade pump under examination here was completely manufactured out of transparent plastic. It it is characterized by the design operating conditions and geometric parameters given in table 1.

Operating conditions		Design parameters			
Q	146.2 m^3/h	D_{ann}	380 mm	β_1	9 deg
H	12.5 m	D_{imp}	240 mm	β_2	35 deg
n	1450 rpm	D_s	100 mm	Θ	332 deg
n_q	43.8 rpm	b	80 mm	K	70 mm

Table 1: Design parameters and operating conditions of test pump

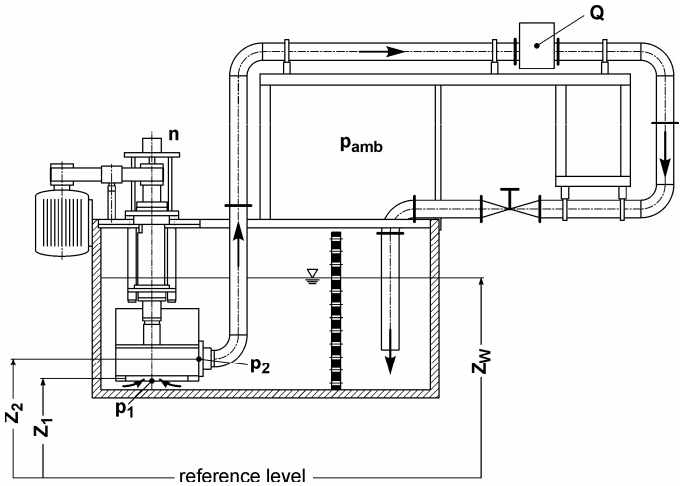

Figure 3: Test stand for submersible pump

As the holding tank has been equipped with new transparent plastic windows, optical access for the PIV-system has been provided. In figure 4 the setup of the PIV-system is shown in a schematic view. Only the pump casing and the impeller with its drive shaft are shown from the pump system.

The ray of the Nd-Yag-Laser system has been extended by optical lenses to a light sheet of about 4 mm thickness which is sent from outside through the optical access to illuminate the particles in the water. Below the water tank a CCD-camera has been mounted on a 2D horizontal traverse system which was placed at a lift table to permit movement of the camera not only in the x- and y-direction but also in the vertical (z-coordinate) direction. The light source was a 20 Hz Dual Nd-Yag-Laser with a maximum pulse energy of 120 mJ per beam and the images have been taken by a CCD camera with a number of 1024 to 1280 pixels and a resolution of 8 bit. The view of the CCD-camera is 57 x 72 mm^2 and is much smaller than the measurement plane of the pump. So the complete picture has been divided into 35 single views which were grabbed in the ascending order as shown in figure 4. As the software of the Dantec PIV-system [8] allows the operation of the 2D traverse system, the grabbing of the individual views has been automated. Each part view has been repeated 20 times in order to carry out a phase averaging. The original impeller position was detected by an inductive impulse sensor. Outgoing from this signal a certain time delay has been calculated to achieve measurements for a special impeller position. To get a complete view of the flow inside the pump, all part views (no. 2 to no. 34) have been combined to only one view with the Matlab software [9]. Doing so, the resolution of the measurements has been strongly increased.

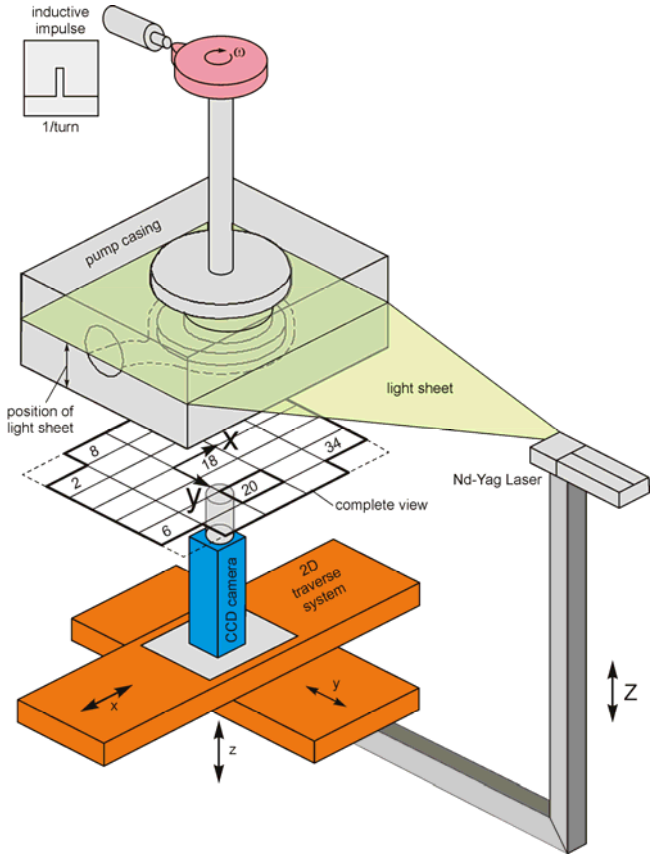

Figure 4: Setup for Particle Image Velocimetry-system

Measurements for the validation of the hydrodynamic forces obtained by numerical simulations were conducted at the same time when the velocity measurements were done. For this, special seats for the roller bearings of the pump shaft have been manufactured. The bearing seats allow an elastic deformation adequate to the loading of the bearings. In figure 5 one of the bearing seats is shown in a front view. The inner annulus carries the bearing and the outer annulus is mounted in the bearing housing. Both rings are connected by four bars which are used for strain measurements to give the loading at the bearings. At all bars two strain gages have been attached at every inner side. A total of 16 strain gages were used for one bearing seat. As can also be taken from figure 5, at every inner wide side of a bar two gages are applied to measure the strain in ξ direction (L) and in ψ direction (C).

ISSN: 1790-5117

ISBN: 978-960-6766-30-5

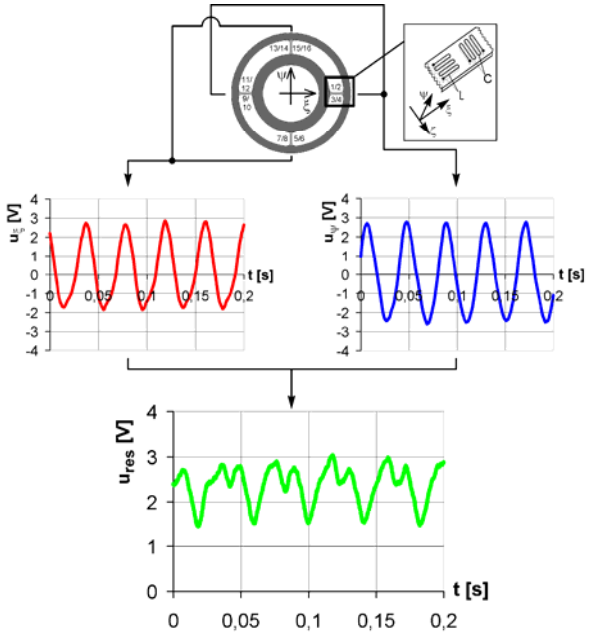

Figure 5: Measured signals for ξ and ψ coordinate

The setup has been calibrated by different masses, which were attached radial at the shaft at an axial position which represents half the blade height. This static calibration provided a linear relationship between the gravitational forces and the resulting voltage. In addition to the static calibration a dynamic calibration was performed. Although the results showed a force orbit which had a slightly elliptic shape the magnitudes of the static calibration were confirmed in the most part.

In figure 5 the measured signals for one operating point of the pump are plotted versus the time. The signals of the strain gages 1-4 and 9-12 were summed up. This gave the voltage, which was induced by the forces acting in ξ-direction. The summation of the signals from the strain gages 5-8 and 13-16 gave the voltage, which was measured for the ψ-direction. A further summation of these both signals provided the voltage U_{res}, which gave the resulting forces acting at the impeller using the calibration curve. By this method, equivalent forces were determined from the measurements, which are responsible for the loading of the bearings. More details about the setup for measurement of hydrodynamic forces can be taken from [10].

4 Results

To evaluate the time-variant velocity field in the pump in a quantitative manner and to compare the measurements to the results of the numerical simulations the measured velocity fields have been transferred to the post processor of Ansys CFX11. The interpolation of the measured velocity field to the computational grid allowed a direct comparison of measured and simulated flow fields. In figure 6 such a qualitative comparison is shown for the impeller position φ = 258 deg as an example. To achieve a quantitative comparison three evaluation lines were defined in the figure, on which the comparison took place. The starting points of the lines are given in the figure as bullets.

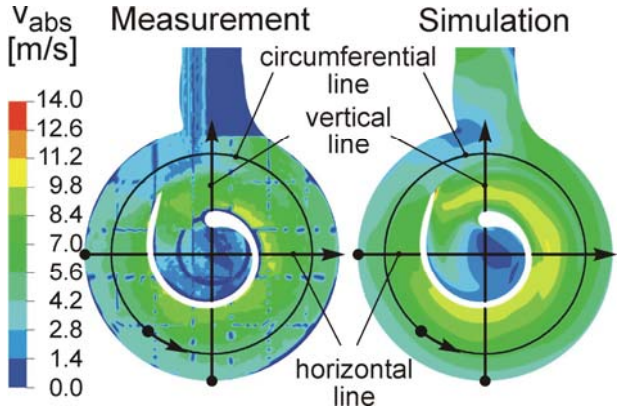

Figure 6: Comparison of absolute velocity fields (design point, φ = 258 deg, mid-span)

In figure 7 the absolute velocities are shown at the three evaluation lines for three operating points at mid-span for the impeller position φ = 258 deg. The best agreement between measurement and simulation has been obtained for the part load operation point. Regarding the design point and the overload operation point, deviations up to 2 m/s can be asserted. The deviations seem to become stronger when approaching to the blade surface. It should be noted here that for these both operating points the entrainment of bubbles might be responsible for a slight corruption of the measurements.

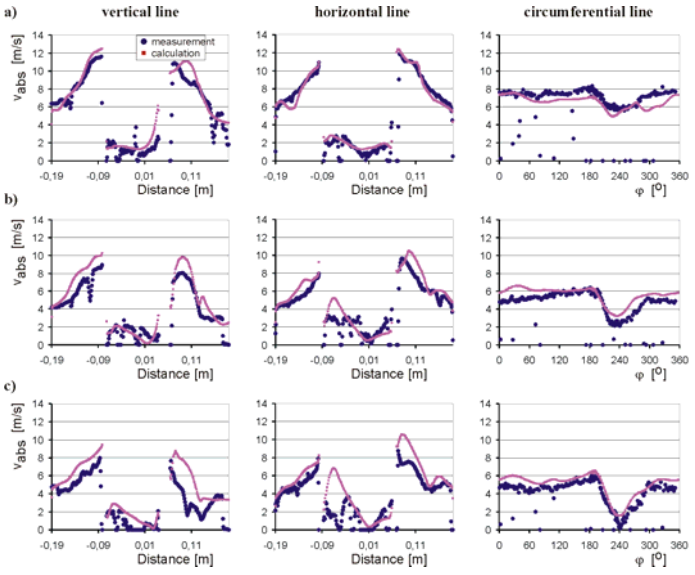

Figure 7: Comparison of abs. velocities for three operating points at mid-span for impeller position φ = 258 deg,
a) part load: Q/Q_{des} = 50%, b) design: Q/Q_{des} = 100%,
c) overload: Q/Q_{des} = 125%

Particularly, in the region of the impeller's suction mouth (-0,05m < Distance < 0,05m) the concordance between measurement and simulation is suboptimal. In

this region the measured velocities are below 4 m/s and a higher outlier percentage has been asserted. This behavior can be explained very easy, because in this region the axial components of the velocities are much stronger than the tangential and radial components which only could be detected with the used arrangement of the PIV-system.

The measured velocity distributions along the circumference of the impeller correspond very well to the calculations for all three operating points. At this evaluation line the deviations are smaller than 1 m/s.

In figure 8 the relative velocities are compared at the three evaluation lines for the design point at mid-span section for the same impeller position (φ = 258 deg). For all three lines a nearly exact agreement between measurement and simulation has been obtained. Even the concordance in the center of the impeller is excellent. The velocity distribution at the circumferential line which was computed from the measurements shows some outlier with high relative velocities. These are the very small or even zero measured absolute velocities emerging at the boundaries of the single views which have been connected together using the Matlab software.

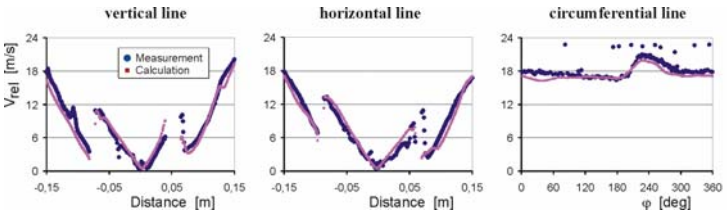

Figure 8: Comparison of relative velocities for the design point at mid-span for φ = 258 deg

For the purpose of a brief statement, it can be annotated that under consideration of remarkable difficulties during the measurements a good concordance between measured and simulated velocity fields has been obtained for all operating points, impeller positions and blade heights under investigation. More detailed information about the PIV-measurements and additional results can be obtained from [11].

In figure 9 the results of the experimental obtained hydrodynamic forces of the single-blade pump are presented in comparison to the ones determined by numerical simulation versus the impeller turning angle. The measurements shown here have been phase averaged over more than 50 impeller revolutions.

For both part load operating points and for the design operating point the ξ-components of the forces are somewhat overestimated for the complete impeller revolution by the numerical model, while the ψ-components meet the measurements very well. Even the locations of the minima and the maxima of the curves have been predicted exactly. The measurements show a tendency of rising forces when the volume flow rate increases from strong part load to design condition. This behavior is reproduced also by the numerical simulation. Overall, the comparison between measurements and numerical results shows a good qualitative agreement, but quantitatively some deviations are observable for the predicted forces.

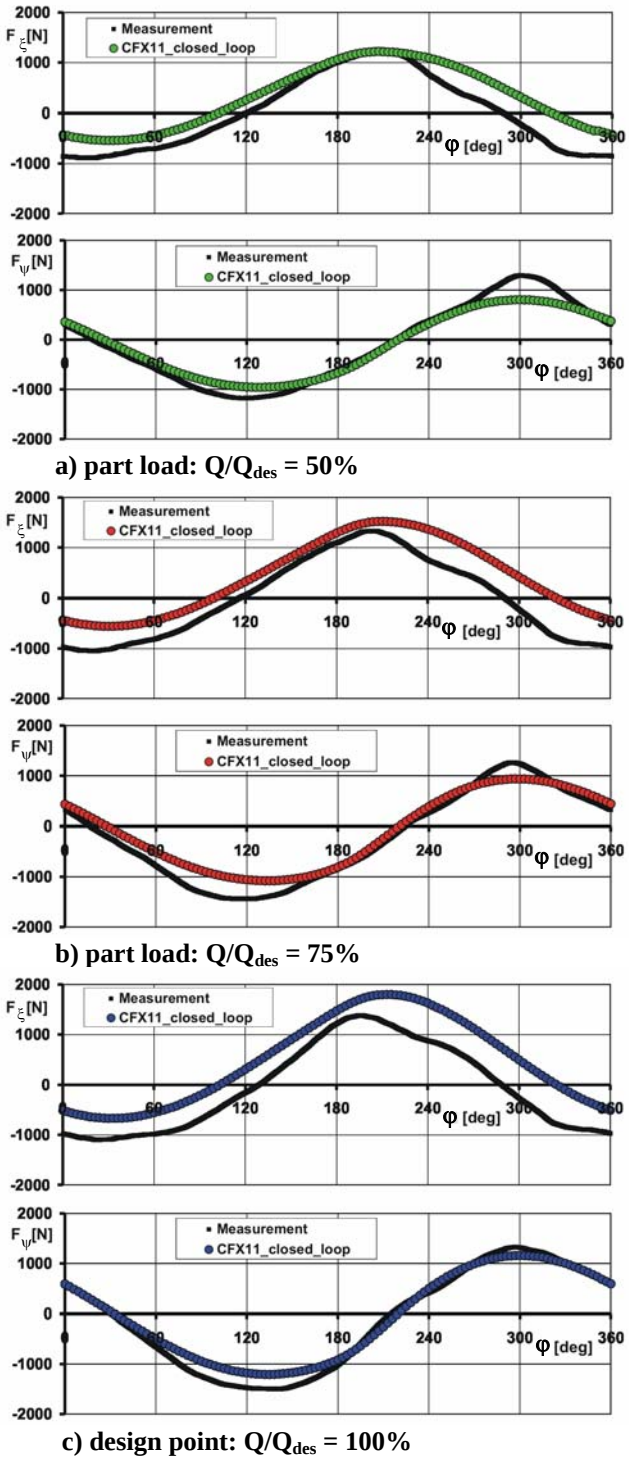

Figure 9: Comparison of measured and simulated transient hydrodynamic forces

5 Conclusions

The time variance of the flow in single-blade sewage water pumps is not yet completely understood. In order to contribute to the understanding of the transient flow

behavior in the present paper numerical and experimental investigations have been performed on the time-variant flow in a single-blade pump. A comparison between the velocity fields obtained by numerical simulation and by measurements using an enhanced optical method shows a good agreement in a wide range of pump operating conditions. Despite some discrepancies at some locations and/or in special operating points the intended validation of the simulation results by the measurements can be regarded as successful. The numerical simulation of the periodic flow in single-blade pumps using commercial Navier-Stokes solvers appears to be reliable. The numerical results give a better insight into the transient flow structure and therefore help to deduce directives for the design of single-blade pumps. In the present paper the transient hydrodynamic forces arising from the pressure field have been computed. Again the validation by measurements shows a good agreement.

.Nomenclature

Arabic letters

A	m^2	Area
D	mm	diameter
$\vec{e}$	-	normal vector
$\vec{F}$	N	force
K	mm	free ball passage
n	rpm	shaft rotational speed
n_q	rpm	specific speed
p	N/m^2	pressure
Q	l/s	volume flow rate
t	s	time
v	m/s	velocity in absolute frame
y+	-	non-dimensional wall distance
x, y, z	m	cartesian coordinates (relative frame)

Greek letters

β	deg	blade angle
Δ	-	difference
φ	deg	angle of rotation, impeller turning angle
Θ	deg	blade wrap angle
μ	kg/(sm)	dynamic viscosity
ω	s^{-1}	angular velocity
ξ, ψ, ζ	m	cartesian coordinates (absolute frame)

Subscripts

amb	ambient
ann	annular
d	discharge
des	design
f	friction
imp	impeller
p	pressure
rad	radial
rel	relative
s	suction
t	total
W	water
1, 2	inlet, outlet

Abbreviations

2D	**2**-**D**imensional
CCD	**C**harge **C**ouple **D**evice
Nd Yag	**N**eodymium-**d**oped **Y**ttrium **a**luminium **g**arnet
SST	**S**hear **S**tress **T**ransport function
URANS	**U**nsteady **R**eynolds **A**veraged **N**avier-**S**tokes equations

References:

[1] Agostinelli, A.; Nobles, D.; Mockridge, C. R., 1960, "An Experimental Investigation of Radial Thrust in Centrifugal Pumps", Transactions of the ASME, Journal of Engineering for Power, Vol. 82, No. 2

[2] Okamura, T., 1980, "Radial Thrust in Centrifugal Pumps with a Single-Vane-Impeller", Bulletin of the JSME 23, No. 180

[3] Aoki, M., 1984, "Instantanous Interblade Pressure Distributions and Fluctuating Radial Thrust in a Single-Blade Centrifugal Pump", Bulletin of the JSME 27, No. 233

[4] Benra, F.-K., Sommer, M., Müller, M., Töws, A., 2004, "Investigation of the Three-Dimensional Time Accurate Flow in Single-Blade Sewage Water Pumps", Proc. of the Fourth South African Conference of Applied Mechanics, SACAM'04, Johannesburg, South Africa

[5] Benra, F.-K., Dohmen, H. J., Sommer, M., 2005, "Periodically Unsteady Flow in a Single-Blade Centrifugal Pump - Numerical and Experimental Results", Proc. of ASME Fluids Engineering Summer Conference, FEDSM2005-77219, Houston, Texas, USA

[6] Benra, F.-K.; Dohmen, H. J.; Schneider, O., 2003, "Investigation on the Unsteady Flow in Radial Waste Water Pumps to Determine the Hydrodynamic Forces", Proceedings of the 5th European Conference on Turbomachinery, Prague, Czech Republic, pp. 551 - 560

[7] Siekmann, H.; Scheffler, T., 1997, "Unsteady Flow Field Investigations by Means of Digital Particle Image Velocimetry", The Fifth Asian International Conference On Fluid Machinery, Seoul, Korea

[8] http://www.dantecdynamics.com/piv/system/software/Index.html

[9] http://www.mathworks.com/products/matlab/description1.html

[10] Benra, F.-K.; Sommer, M., 2005, "Comparison of Calculated and Measured Hydrodynamic Forces of a Centrifugal Sewage Water Pump", Proceedings of 1st Intern. Conference on Experiments / Process / System Modeling / Simulation / Optimization, Athens, Greece

[11] Benra, F.-K., Dohmen, H. J., Zwingenberg, M., 2006, "Comparison of Experimental and Numerical Obtained Velocity Fields in a Single-Blade Centrifugal Pump", Forum on Fluid Machinery, FEDSM2006-98351, Miami, Florida, USA